THE JOURNAL OF BIOLOGICAL CHEMISTRY Vol. 278, No. 27, Issue of July 4, pp. 24874–24880, 2003
*Printed in U.S.A.*

# Dentin Sialophosphoprotein Knockout Mouse Teeth Display Widened Predentin Zone and Develop Defective Dentin Mineralization Similar to Human Dentinogenesis Imperfecta Type III*

Received for publication, April 14, 2003
Published, JBC Papers in Press, April 29, 2003, DOI 10.1074/jbc.M303908200

**Taduru Sreenath‡§, Tamizchelvi Thyagarajan‡, Bradford Hall‡, Glenn Longenecker‡, Rena D'Souza¶, Sung Hong¶, J. Tim Wright‖, Mary MacDougall**, John Sauk‡‡, and Ashok B. Kulkarni‡¶¶**

*From the ‡Functional Genomics Unit and Gene Targeting Facility, NIDCR, National Institutes of Health, Bethesda, Maryland 20892, ¶University of Texas Health Science Center at Houston, Houston, Texas 77030, ‖University of North Carolina, Chapel Hill, North Carolina 27599, **University of Texas Health Science Center at San Antonio, San Antonio, Texas 78229, and ‡‡University of Maryland at Baltimore, Baltimore, Maryland 21201*

**Dentin sialophosphoprotein (*Dspp*) is mainly expressed in teeth by the odontoblasts and preameloblasts. The Dspp mRNA is translated into a single protein, Dspp, and cleaved into two peptides, dentin sialoprotein and dentin phosphoprotein, that are localized within the dentin matrix. Recently, mutations in this gene were identified in human dentinogenesis imperfecta II (Online Mendelian Inheritance in Man (OMIM) accession number 125490) and in dentin dysplasia II (OMIM accession number 125420) syndromes. Herein, we report the generation of Dspp-null mice that develop tooth defects similar to human dentinogenesis imperfecta III with enlarged pulp chambers, increased width of predentin zone, hypomineralization, and pulp exposure. Electron microscopy revealed an irregular mineralization front and a lack of calcospherites coalescence in the dentin. Interestingly, the levels of biglycan and decorin, small leucine-rich proteoglycans, were increased in the widened predentin zone and in void spaces among the calcospherites in the dentin of null teeth. These enhanced levels correlate well with the defective regions in mineralization and further indicate that these molecules may adversely affect the dentin mineralization process by interfering with coalescence of calcospherites. Overall, our results identify a crucial role for Dspp in orchestrating the events essential during dentin mineralization, including potential regulation of proteoglycan levels.**

Tooth development depends on reciprocal interactions between oral epithelium and mesenchyme (1). The mesenchyme-derived odontoblasts secrete several collagenous and non-collagenous proteins to form a unique extracellular matrix (2). Among the non-collagenous proteins, dentin sialoprotein (Dsp)[1] and dentin phosphoprotein (Dpp) are highly tooth-specific and are believed to play a crucial role in converting predentin to form mineralized dentin. These two proteins are derived from the cleavage of a 940-amino acid polypeptide, dentin sialophosphoprotein (Dspp) (3). The *Dspp* gene consists of five exons spanning 16 kb and is transcribed as a 4.4-kb mRNA (4). mRNA for *Dspp* is expressed predominantly by odontoblasts and transiently by preameloblasts (5–7). Recently, however, low levels of *Dspp* have been observed in the ear and in bone (8, 9). The Dsp, the amino-terminal part of Dspp, is a sialic acid-rich and glycosylated protein that shares similarities with the other sialoproteins, including bone sialoprotein, dentin matrix protein-1, and osteopontin. The Dpp, a highly phosphorylated protein with repeats of aspartic acid and phosphoserine, is thought to play a key role in the nucleation of hydroxyapatite formation during dentin calcification (10–12). Because of its restricted expression and its physical localization on the human chromosome 4q within the dentinogenesis imperfecta (DGI)-II locus (13, 14), *Dspp* was implicated as a potential candidate gene for this disorder. The other important genes involved in biomineralization mapped to this region of chromosome 4q include dentin matrix protein-1, bone sialoprotein, and osteopontin.

DGI, an autosomal dominant disorder of the tooth that primarily affects dentin biomineralization, is classified into three subtypes, based on the clinical features; type I is the least severe and type III is the most severe (15). DGI-I is associated with osteogenesis imperfecta, whereas the more severe forms (DGI-II and DGI-III) are restricted to the dentin. Opalescent dentin with obliterated pulp chambers are the characteristic features in DGI-II (16). The teeth of patients with DGI-III are referred to as 'shell teeth,' in which the dentin mineralization does not occur after mantle dentin is formed. Radiographically, the pulp cavities in these teeth appear as enlarged pulp chambers along with high incidence of pulp exposures (17, 18).

Recently, several mutations in the *Dspp* gene have been identified in families with DGI-II disorder. These mutations include a C to T transition at the end of the third exon (Gln45stop) resulting in a premature termination of Dspp protein (19), a G to A transition mutation in intron 3 (splice donor site) causing exon skipping, and Pro17Thr and Val18Phe transitions (8). Dentin dysplasia-II, another human disorder of

* The costs of publication of this article were defrayed in part by the payment of page charges. This article must therefore be hereby marked "*advertisement*" in accordance with 18 U.S.C. Section 1734 solely to indicate this fact.

§ To whom correspondence may be addressed: 30 Convent Dr., Room 527, Bethesda, MD 20892. Tel.: 301-402-5061; Fax: 301-435-2888; E-mail: tsreenat@mail.nih.gov.

¶¶ To whom correspondence may be addressed: 30 Convent Dr., Room 527, Bethesda, MD 20892. Tel.: 301-435-2887; Fax: 301-435-2888; E-mail: akulkarn@mail.nih.gov.

[1] The abbreviations used are: Dsp, dentin sialoprotein; Dpp, dentin phosphoprotein; Dspp, dentin sialophosphoprotein; DGI, dentinogenesis imperfecta; ES, embryonic stem; GAG, glycosaminoglycans; RT, reverse transcription/transcriptase.

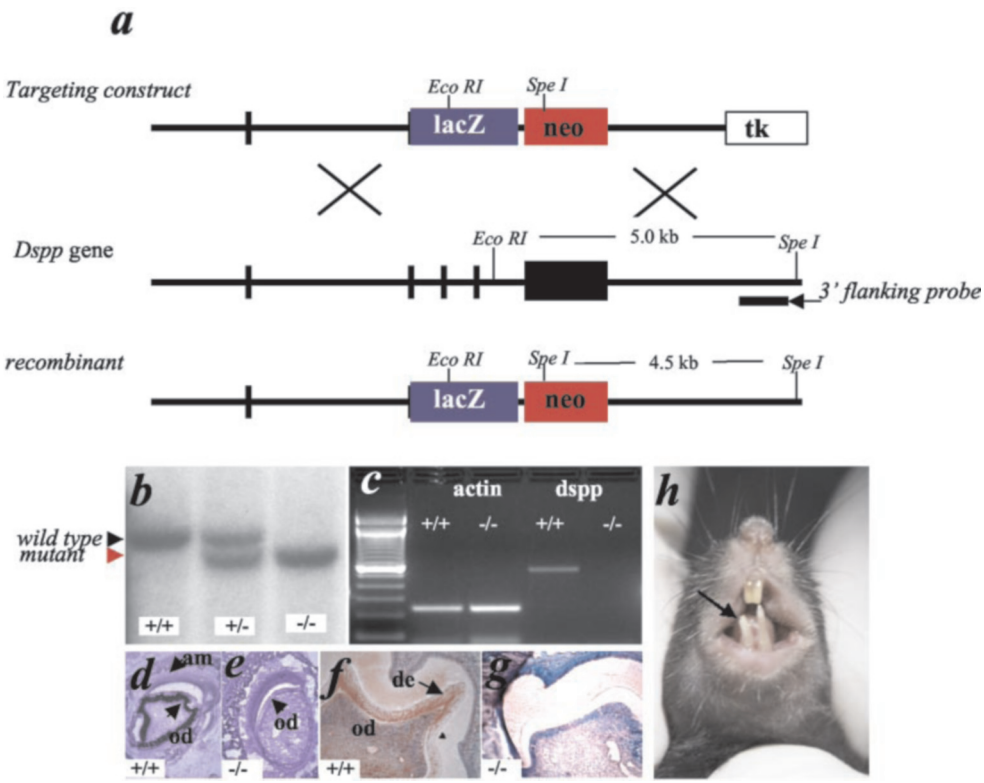


FIG. 1. **Generation of Dspp−/− mice.** *a*, structure of the wild-type *Dspp* gene, the targeting construct, and location of 3′ flanking probe to confirm targeted disruption in both ES cells and mice. Homologous recombination at the *Dspp* locus will result in a smaller (4.5 kb)-than-endogenous genomic DNA fragment (5.0 kb) upon digestion with *Spe*I + *Eco*RI. The *vertical bars* and *filled boxes* represent exons. *b*, Southern blot analysis of wild-type (+/+), heterozygous (+/−), and homozygous (−/−) mouse tail DNA hybridized to the 3′-flanking probe, showing the presence of the smaller fragment indicating targeted disruption of *Dspp* locus. *c*, a lack of *Dspp* expression in P6 *Dspp*−/− mouse molars confirmed by RT-PCR. *d* and *e*, *in situ* hybridization with digoxigenin-labeled antisense *Dspp* RNA on the frozen sections from wild-type (*d*) and *Dspp*−/− P6 (*e*) mice. The odontoblasts in *Dspp*−/− teeth show lack of *Dspp* mRNA expression (*arrowheads*). *f* and *g*, immunodetection of *Dspp* protein using anti-Dspp polyclonal antibodies on the decalcified frozen sections of P6 mice, showing absence of Dspp protein in the dentin of *Dspp*−/− teeth. *h*, 1-year-old *Dspp*−/− mouse with broken mandibular incisor (*black arrow*). *am*, ameloblasts; *od*, odontoblasts; *de*, dentin.

dentin mineralization, is similar to DGI-II and is attributed to a Tyr6Asp protein transition mutation in the hydrophobic core sequence of the *Dspp* gene. This mutation disabled the entry of Dspp into the endoplasmic reticulum (20). All these mutations indicate a potential function for Dspp in tooth mineralization. To characterize the molecular events that control dentin mineralization during normal tooth development and disease, we have deleted the entire Dspp coding region in embryonic stem (ES) cells and generated *Dspp*−/− mice. These null mice displayed an enlarged pulp cavity, widened predentin zone, decreased dentin width, and high incidence of pulp exposures similar to that in DGI-III. In addition, these mice showed an increased accumulation of biglycan and decorin within the widened predentin and scalloped (void spaces) regions in the dentin, correlating well with defective mineralization.

## MATERIALS AND METHODS

*Generation of Dspp−/− Mice*—*Dspp* genomic clones from a *129/SvJ* mouse genomic library were cloned and characterized as reported previously (4). The targeting vector was constructed by standard recombinant DNA techniques; the *Nsi*/*Eco*RV region of exons 2–5 spanning the entire coding region of *Dspp* was replaced by a promoterless β-galactosidase gene with simian virus 40 polyadenylation sequences (21) followed by a neomycin-resistance and thymidylate kinase cassettes. The targeting vector was linearized with *Not*I and electroporated into 129/SvJ R1 embryonic stem cells. ES-cell clones that survived G-418 and ganciclovir selection were evaluated for homologous recombination by Southern blot analysis. ES cells were injected into C57BL/6 blastocysts and the chimeric mice produced were mated to C57Bl/6 female mice to derive heterozygotes. Heterozygous mice were then interbred to obtain homozygous mice and maintained as homozygotes. The null mice were viable and able to reproduce normally. All mice were housed according to National Institutes of Health guidelines.

*In Situ Hybridization*—Digoxigenin-11-dUTP-labeled sense and antisense riboprobes were generated from *Dspp* exons 3 and 4 (pSX1.7) and hybridized to the frozen tissue sections obtained from 6-day-old mouse teeth as described previously (22).

*Microradiography*—Wild-type and Dspp−/− mice were sacrificed, and the mandibles were separated and radiographed using a Faxitron MX20 Specimen Radiography System (Faxitron X-ray Corp., Wheeling, IL) at energy settings 120 s at 15 kV (22). The images were captured on X-OMAT TL film (Eastman Kodak).

*Scanning and Transmission Electron Microscopy*—The jaws were dissected from the control and mutant mice and immersed in a 2.5% glutaraldehyde and 2% paraformaldehyde buffered solution, pH 7.4, for 12 h. The jaws are then transferred to a 0.1 M cacodylate buffer solution, pH 7.4. The teeth were dissected from the jaws using a dissecting microscope and prepared for analysis using the following techniques. Teeth were fractured and the samples mounted with the fractured surface facing, coated with Au-Pd using a sputter coater, and examined in a JEOL 6300 scanning electron microscope. After fixation, whole mandibles were glued to a glass slide and polished to an optically flat surface (1/4 μm) using an automatic polisher. The jaws were removed from the glass slide using acetone and rinsed with ethanol and $dH_2O$, air dried, mounted on a carbon stub, and carbon coated. The samples were examined using a JEOL 6300 scanning electron microscope fitted with a backscatter detector (25-mm working distance, 15 kV). Small pieces of the incisors and molars were dissected from the teeth and osmicated before serial dehydration in ethanol. After dehydration, the samples were embedded in epoxy and then sectioned with an ultramicrotome. Sections were floated onto Formvar grids and stained with uranyl citrate and lead acetate. The samples were examined with a Phillips CM12 transmission electron microscope.

*Histology and Mineral Staining*—The skulls from euthanized wild-type and *Dspp*−/− mice were dissected and fixed in 4% paraformaldehyde. The fixed skulls were processed, embedded in methyl methacrylate for 150-μm sections using an ISOMET low speed saw (Buehler, Lake Bluff, IL), and stained for calcium by von Kossa's method. For

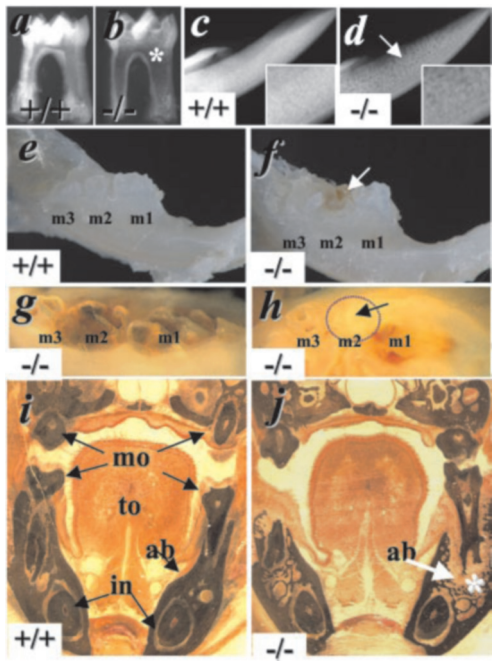


FIG. 2. **Tooth abnormalities in 1-year-old Dspp−/− mice.** Extracted first molars from wild-type (*a*) and *Dspp*−/− (*b*) mice, showing enlarged pulp cavity (*) by microradiography. Similarly, decreased mineral density was observed in the incisors (*arrow*) of the *Dspp*−/−mice (*d*). Prominent globular mineralized zones (*arrow*) in *Dspp*−/− incisors at the incisal end are shown as *insets* in *d*. Molars of *Dspp*−/− mice (*f–h*) show discoloration (*arrow*) and severe attrition, leading to the complete disappearance of tooth crown (*dotted circle*). Frontal sections of wild-type (*i*) and *Dspp*−/− (*j*) skulls showing the distribution of calcium staining, abnormal molar pulp cavity and resorption of the bone surrounding the teeth (*). *ab*, alveolar bone; *to*, tongue; *in*, incisors; *m1*, molar 1; *m2*, molar 2; *m3*, molar 3; *mo*, molars.

general histology and for immunohistochemical analysis, mandibles were dissected, fixed in 4% paraformaldehyde, decalcified in 0.1 M EDTA-sodium phosphate buffer for 3 weeks, dehydrated, and embedded in paraffin wax.

*Glycosaminoglycans Staining*—Frozen frontal sections (6 μm) from 6 day-old wild-type and *Dspp*−/− mouse heads were cut and treated with 100 μl of 0.1units/ml chondroitinase ABC (EC 4.2.2.4; Seikagaku America, Falmouth, MA) for 2 h at 37 °C to digest the glycosaminoglycans (GAGs). Digested and undigested tooth sections were stained for the presence of sulfated GAGs with Alcian blue reagent containing 0.5 M magnesium chloride at pH 0.5 according to the method of Smith *et al.* (23).

*RNA Extraction and RT-PCR*—Incisors from adult wild-type and mutant mice were dissected out and split sagittally into two halves using a stainless steel mini-scalpel (Cincinnati Surgicals, Cincinnati, OH) and pulp was dissociated overnight at 37 °C with collagenase (Worthington) (5 mg/ml in F16 media supplemented with 20% fetal bovine serum). The teeth were washed several times with sterile phosphate-buffered saline to remove all the pulp cells. RNA was extracted by lysing the odontoblasts that were trapped in the dentin using a Micro RNA Isolation kit (Stratagene). RT-PCR was performed using Ready-To-Go RT-PCR beads (Amersham Biosciences) according to the manufacturer's instructions using the following primers: dspp (forward (F)), 5′-GGC ATA ATC AAA ACA CCG CTG C-3′; (reverse (R)), 5′-GGG GAA ATA GGG AAA TGA CAA AGG-3′; coll-I (F), 5′-ACC ATC TGG CAT CTC ATG GC-3′; (R), 5′-GCA ACA CAA TTG CAC CTG AGG-3′; biglycan (F), 5′-ACC TGT CCC CTT CCA TCT T-3′; (R), 5′-CCG TGT GTG TGT GTG TGT GT-3′; decorin (F), 5′-CCA ACA TAA CTG CGA TCC CT-3′; (R), 5′-TGT CCA AGT GGA GTT CCC TC-3′; mmp-3 (F), 5′-AGT GGA TCT TCG CAG TTG GAA TTT GAC-3′; (R), 5′-GTG TAA GCT ACA CAG TGC TTC TGA AC-3′; β-actin (F), 5′-GTG GGC CGC TCT AGG CAC CA-3′; (R), 5′-CGG TTG GCC TTA GGG TTC AGG GGG-3′; and gapdh (F), 5′-CCA TCA CCA TCT TCC AGG AG-3′; (R), 5′-GCA TGG ACT GTG GTC ATG AG-3′. The PCR products were electrophoresed on a 2% agarose gel.

*Immunohistochemistry*—Immunodetection of Dspp, biglycan, and decorin was performed on 5-μm thick paraffin sections. The sections were deparaffinized in xylene and rehydrated in a descending ethanol series. For biglycan and decorin immunostaining, the sections were treated with 100 μl of 0.1 units/ml chondroitinase ABC for 2 h at 37 °C to digest the GAGs before antibody addition. The tissues were incubated with rabbit polyclonal anti-Dsp (LF-153), anti-biglycan (LF-106), or anti-decorin (LF-113) (24) antibodies at 1:1000 dilution. The immune complexes were incubated with peroxidase-conjugated secondary antibodies. The peroxidase reaction in the immune complexes was visualized by a chromogen substrate 3-amino-9-ethyl carbazole reaction according to the manufacturer's instructions (Histostain plus kit; Zymed Laboratories Inc.).

## RESULTS

*Gene Targeting Strategy and Generation of Dspp−/− Mice*—We have previously reported cloning and characterization of the mouse *Dspp* gene (4). The targeting construct was designed to replace the entire coding region of *Dspp* with the promoterless β-galactosidase gene (Fig. 1*a*). The successful disruption of the *Dspp* gene was confirmed by Southern hybridization using a 3′-flanking probe (data not shown). The targeted ES cells clones were injected into blastocysts to generate the chimeras. The high-percentage chimeras were mated with wild-type mice to obtain heterozygous mice. Genotypes of these mice were confirmed by Southern hybridization using a 3′-flanking probe (Fig. 1*b*), and the lack of gene expression was analyzed by RT-PCR (Fig. 1*c*) and by *in situ* hybridization using a *Dspp* exon 3–4–specific riboprobe (Fig. 1, *d* and *e*). Dspp protein expression was analyzed by immuno-histochemistry (Fig. 1, *f* and *g*). The null mice did not show any overt tooth phenotype until 2–3 months of age. Occasionally, the incisors appeared broken in some older null mice (Fig. 1*h*).

*Dspp−/− Mice Exhibit Tooth Mineralization Defects*—Qualitative differences in mineral density between the control teeth and *Dspp*−/− molars and incisors (Fig. 2, *a–d*) were observed in 70-day-old mice. The pulp chambers in the molars from mutant mice showed significant enlargement (Fig. 2, *a* and *b*). Mineralization defects in the *Dspp*−/− mouse incisors were characterized as globular dentin with extensive inter-globular regions. The presence of globular dentin, a marker of abnormally mineralized dentin, was prominent at the incisal end of the *Dspp*−/− mice (Fig. 2*d*) compared with the wild-type incisors (Fig. 2*c*). Early signs of pulp exposure were observed in the molars of *Dspp*−/− mice from about 2–3 months of age (Fig. 2 *e*, *f*). Pulp exposures seemed to occur randomly among all the molars. An increased incidence of pulp degeneration was observed in older *Dspp*−/− mice. Because of pulp exposure and severe attrition, the tooth crowns were worn to the level of the gingiva (Fig. 2, *g* and *h*). The molars from these mutant mice that are affected with pulp exposure also displayed relatively shortened tooth roots. The discoloration of teeth observed in the mutant mice was caused by pulp exposure followed by increased pulp degeneration (Fig. 2, *e–h*). Incisors of *Dspp*−/− mice did not exhibit either attrition or pulp exposures. Distribution of calcium in the teeth and surrounding alveolar bone, examined qualitatively by von Kossa's staining, displayed no significant differences in the mutant mouse (Fig. 2, *i* and *j*). The alveolar bone resorption was evident around the tooth root only in the *Dspp*−/− teeth that were affected by pulp exposure as a result of hypomineralization of dentin. It has been reported previously that alveolar bone resorption occurs as a result of inflammation in experimentally induced pulp infections in rodents (25).

*Reduced Thickness of Dentin, Widened Predentin, and Irregular Mineralization Front in Dspp−/− Teeth*—Scanning electron microscopy of fractured Dspp−/− teeth showed an increased predentin region (Fig. 3, *a* and *b*) with the scalloped (irregular) dentin-predentin border (Fig. 3, *c* and *d*). The irregular mineralization front observed in the null mice was caused

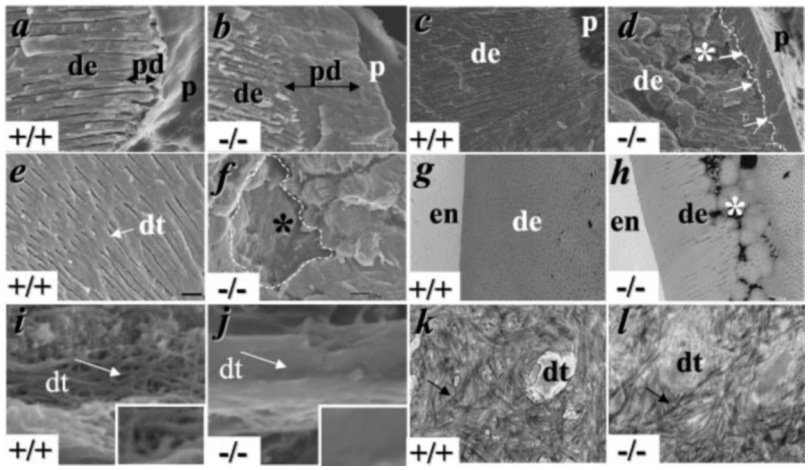


FIG. 3. **Widened predentin and defective dentin mineralization in the Dspp−/− mice.** Scanning, backscatter, and transmission electron microscopy analyses of the molars from wild-type (*a*, *c*, *e*, *g*, *i*, *k*) and *Dspp*−/− (*b*, *d*, *f*, *h*, *j*, *l*) teeth showing enlarged predentin (*b*) and irregular mineralization front (*d*) (*white arrows*), which often appears as pits (*) because of lack of coalescence of calcospherites, the void spaces in the dentin (*). Irregular dentinal tubules and scalloped dentin (void spaces as indicated by *) are prominent in the *Dspp*−/− teeth (*f*). *g* and *h*, backscatter scanning electron microscopy showing lack of coalescence of calcospherites in the dentin region with increasing number of void spaces (*) in the *Dspp*−/− mice (*h*). *i* and *j*, higher magnification of the predentin region showing a lack of organized network in the tubular and inter-tubular regions in the Dspp−/− teeth (*j* and *inset*). *k* and *l*, transmission electron microscopy analysis of decalcified teeth from wild-type (*k*) and *Dspp*−/− (*l*) mice shows no obvious differences in the (*arrows*) organization of collagen fibrils/bundles (*arrow*). *de*, dentin; *en*, enamel; *p*, pulp; *pd*, predentin; *dt*, dentinal tubules.

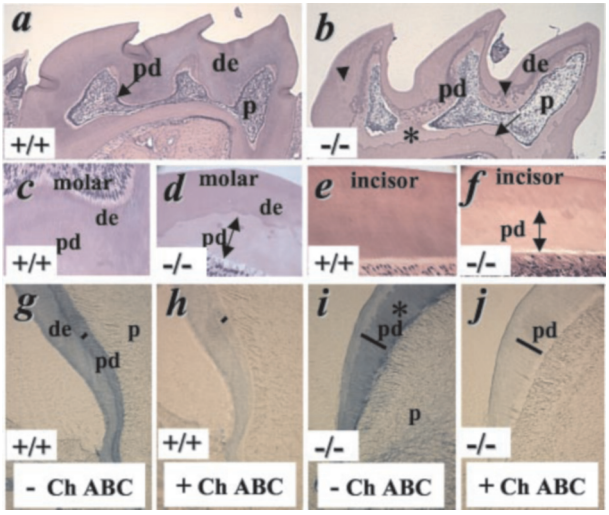


FIG. 4. **General histology and presence of GAGs in the widened predentin.** Dspp−/− molars (*b*) show widened predentin (*) and irregular mineralization (*arrow*) with globular dentin in the predentin (arrowheads). *c–f*, higher magnifications of wild-type (*c* and *e*) and *Dspp*−/− (*d* and *f*) molars (*c* and *d*) and incisors (*e* and *f*) showing widened predentin. *g–j*, frozen tooth sections from 6-day-old wild-type (*g* and *h*) and *Dspp*−/− (*i* and *j*) mice were stained for GAG containing proteoglycans with Alcian blue before (*g* and *i*), and after (*h* and *j*) chondroitinase ABC treatment. The dentin and predentin region indicate the disappearance of blue staining in the predentin after chondroitinase ABC treatment. *de*, dentin; *p*, pulp; *pd*, predentin.

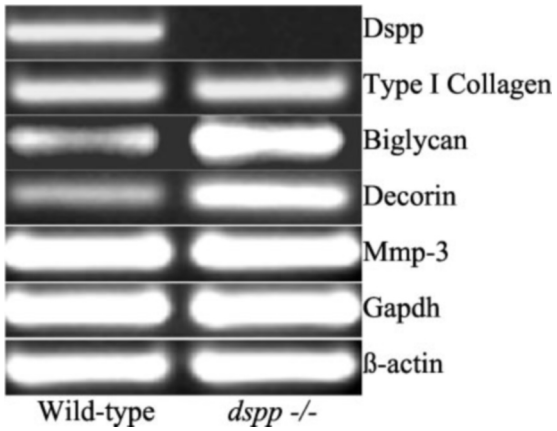


FIG. 5. **Altered gene expression in the Dspp−/− odontoblasts.** RT-PCR analysis showing increased levels of biglycan, decorin, and unaltered type I collagen and mmp-3 mRNA expression in *Dspp*−/− odontoblasts. β-Actin and gapdh were used as controls. *Dspp* mRNA was not amplified in *Dspp*−/− teeth.

by a lack of proper coalescence of calcospherites. Void spaces and scalloped dentin in the mineralized dentin were also observed in *Dspp*−/− teeth (Fig. 3, *e–h*). The widened predentin in the *Dspp*−/−mouse teeth frequently lacked a visible dense collagenous network lining the dentinal tubules, and the well-organized intertubular dentin was absent because of masking of the fibers by increased hydration or by proteins (Fig. 3, *i* and *j*). Type I collagen fibrils, the most abundant component of the dentin extracellular matrix, appeared normal in the *Dspp*−/− dentin and were arranged in a pattern similar to that seen in the wild-type tissue (Fig. 3, *k* and *l*). The size of the collagen fibers and the cross-striation dimension (control, ~67 nM; *Dspp*−/−, ~60 nM from transmission electron microscopy measurements) were similar and appeared normal in the *Dspp*−/− and control mice.

*Increased Proteoglycans in Widened Predentin of the Dspp*−/− *Mice*—Histological analysis revealed a marked reduction in the width of the mineralized dentin and an increase in the width of the predentin. The unmineralized layer (predentin) of molar (Fig. 4, *a–d*) and incisor (Fig. 4, *e* and *f*) dentin was similar to the widened predentin in human teeth affected with DGI-III (17, 18). During active dentinogenesis in molars, the predentin layer was initially wide and subsequently reduced to minimum at the coronal region of the mineralized dentin. Proteoglycans are among the few molecules that are identified in the dentin extracellular matrix and are synthesized and secreted by the odontoblasts. Prominent Alcian blue staining, which binds proteoglycans, was observed in the widened predentin region in the null teeth (Fig. 4*i*), and was lost upon chondroitinase ABC treatment (Fig. 4*j*), indicating increased levels and wider distribution of proteoglycans in the predentin of the null mice relative to the control mice.

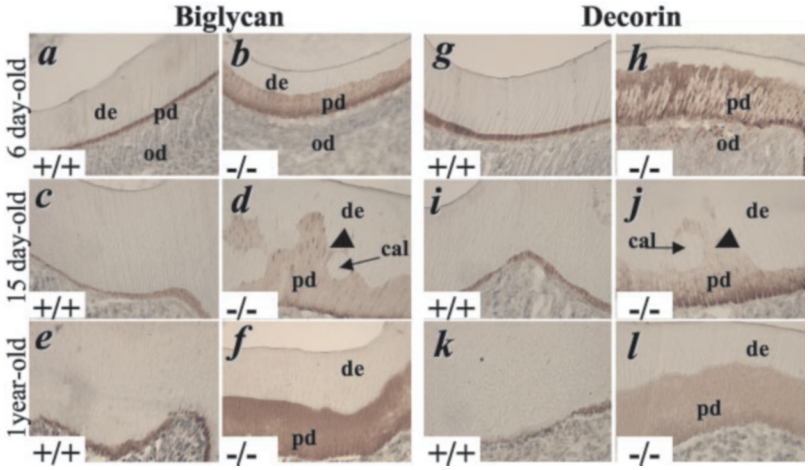


FIG. 6. **Developmental expression of biglycan and decorin in the teeth using polyclonal antibodies.** Expression of biglycan in P6 (*a* and *b*), P15 (*c* and *d*), and 1-year-old (*e* and *f*) wild-type (*a*, *c*, *e*) and *Dspp*−/− (*b*, *d*, *f*) teeth showing increased accumulation in the predentin region and around the calcospherites (*cal*) in the dentin (*arrowhead*) of *Dspp*−/− teeth. Similarly, the expression of decorin in P6 (*g* and *h*), P15 (*i* and *j*), and 1 year-old (*k* and *l*) wild-type (*g*, *i*, *k*) and *Dspp*−/− (*h*, *j*, *l*) teeth indicates elevated levels in the predentin region of *Dspp*−/− teeth. *de*, dentin; *od*, odontoblasts; *pd*, predentin, *cal*, calcospherites.

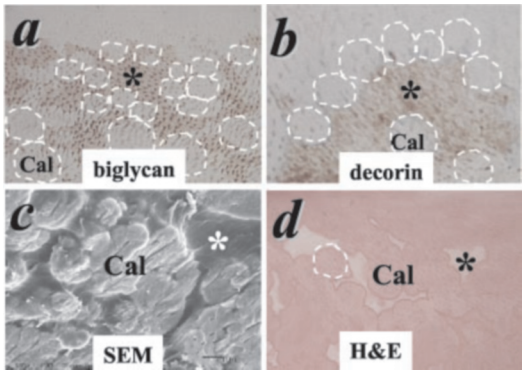


FIG. 7. **Accumulation of biglycan and decorin in the inter-calcospherite spaces of the Dspp−/− teeth.** Immunostaining of mouse tooth sections with biglycan (*a*), and decorin (*b*) shows accumulation around calcospherites. Scanning electron microscopy of the fractured teeth (*c*) showing the void spaces (*) in the dentin similar to the lightly stained regions (unmineralized) in hematoxylin and eosin-stained teeth (*d*). *cal*, calcospherites.

*Increased Expression of Biglycan and Decorin in the DSPP−/− Odontoblasts*—Expression of dspp, type I collagen, biglycan, decorin, mmp-3, gapdh, and β-actin was analyzed by RT-PCR in the enriched odontoblast population from wild-type and Dspp−/− incisors (Fig. 5). Biglycan and decorin, found in dentin and rich in GAG, belong to a family of small leucine-rich proteoglycans that are predominantly expressed in skin, bone, and teeth (26–30). Small leucine-rich proteoglycans have a well established role in collagen fibrillogenesis and collagen packing (31). Biglycan and decorin mRNA expression was increased in the Dspp−/− compared with the wild-type teeth. Type I collagen is one of the major components to play an essential role in the mineralization and structural integrity of dentin. The expression of type I collagen was not altered in the null teeth. It is believed that the removal of sulfated GAGs from proteoglycans is required to mineralize the matrix, because they mask the mineral nucleator sites on the collagen fibrils. Expression of matrix metalloproteinase-3, which is implicated in the degradation of GAGs from chondroitin 4-sulfate/dermatan sulfate-containing proteoglycans in the predentin and subsequently increases keratan sulfate-containing proteoglycans near the distal part of predentin to form the mineralization front (32), was not altered in the *Dspp*−/− teeth. The expression of gapdh and β-actin, housekeeping genes, was used as control in these experiments.

*Increased Biglycan and Decorin May Be Associated with Mineralization Defects in Dspp−/− Teeth*—To examine whether biglycan and decorin are involved in mineralization mechanisms, we analyzed their levels in the *Dspp*−/− and wild-type mouse teeth. In 6-day-old *Dspp*−/− mouse teeth, strong immunoreactivity for biglycan and decorin was observed in the predentin (Fig. 6, *b* and *h*) compared with controls (Fig. 6, *a* and *g*). Similarly, increased immunoreactivity of biglycan and decorin was also observed in 15-day-old (Fig. 6, *d* and *j*) and 1-year-old (Fig. 6, *f* and *l*) mouse teeth without pulp exposure. The prominent irregularity of the mineralization front observed in the teeth of *Dspp*−/− mice can be correlated with the lack of coalescence of the calcospherites in the mineralization process. Interestingly, high levels of biglycan and decorin were accumulated in the void spaces in the dentin (Fig. 7, *a* and *b*) where the calcospherites are not properly coalesced (Fig. 7, *c* and *d*). These data suggest that increased localization of biglycan and decorin in the predentin and dentin may potentially interfere with the mineral nucleation and subsequent coalescence of calcospherites in forming a defined mineralization front.

## DISCUSSION

Biomineralization of dentin extracellular matrix requires complex interactions among several collagenous and non-collagenous molecules. Dspp, an important molecule in the dentin, is cleaved into Dsp and Dpp and localized predominantly in the dentin. Based on its gene expression and localization within the DGI-II locus on human chromosome 4q, Dspp is implicated as a critical molecule in converting predentin to dentin, and recently observed mutations in the Dspp gene in DGI patients further support its potential role in dentin mineralization. The primary phenotypic features seen in DGI-II and DGI-III are defective dentin that had been largely attributed to functionally defective or reduced levels of the *Dspp* products, Dsp and Dpp (33), or to mutations in the *Dspp* gene (8, 19). These disorders also show significant phenotypic variations and degrees of severity. It has been suggested that the DGI-III phenotype could develop because of the homozygosity of the DGI-II mutation (17, 34). To analyze the precise functions of Dspp in tooth mineralization, we generated Dspp−/− mice, which develop defective and reduced dentin mineralization and pulp exposures similar to those of DGI-III patients.

Mineralization of dentin is initiated at the predentin-dentin interface and forms the mineralization front, characterized by the presence of multiple globular mineral foci "calcospherites." These calcospherites grow and coalesce with the adjacent calcospherites to form a relatively uniform mineralization front. A lack of proper coalescence of calcospherites in the dentin, an irregular mineralization front, and scalloped dentin similar to those of the DGI-III patients (18) were observed in the *Dspp*−/− mice. Type I collagen is the main component secreted by the odontoblasts, which form a visible network around the

dentinal tubules in the peritubular region and in the intertubular predentin region. Such a network was not visible in the null mice because of increased hydration. Similar observations were made earlier in DGI (35). However, type I collagen bundles and organization in the dentin extracellular matrix seemed normal in the Dspp-null mice. The mRNA levels were also unaltered in these mice, indicating that the mineralization defects observed in the teeth of *Dspp*−/− mice were independent of collagens.

During dentin mineralization, phosphoproteins, sialoproteins, proteoglycans and growth factors interact with each other to form predentin, which subsequently mineralizes to form dentin. A number of biochemical and immunohistochemical studies have demonstrated the presence of chondroitin sulfate and GAGs in calcified tissues, including teeth (27). Proteoglycans belong to a family of glycoconjugates and contain one or more GAGs covalently attached to the protein core. The GAGs are known to bind calcium and interact with hydroxyapatite and are readily detectable by Alcian blue staining (23, 28, 36). Wider distribution of GAG staining observed in the predentin region of *Dspp*−/− mice indicated the presence of proteoglycans. Among small leucine-rich proteoglycans, decorin and biglycan have been well characterized for their presence in the tooth. In mouse teeth, decorin was localized in odontoblasts, predentin, and dentin and biglycan in odontoblasts and predentin (37). *In vitro* studies have implied that decorin and biglycan play a crucial role in fibril growth and assembly. Decorin binds to specific sites of collagen fibrils very near the putative hydroxyapatite nucleation site, a "gap" zone in which mineral is preferentially deposited in the early stage of mineralization (38, 39). Decorin also functions as an inhibitor of mineralization during primary ossification of rat embryo bones (40). Interestingly, biglycan facilitates the initiation of apatite formation and inhibits the growth of apatite (41). Overall, it seems that decorin and biglycan may have distinct roles in the mineralization process. The teeth of biglycan- and decorin-null mice also show widened and porus dentin and changes in collagen fibril diameter, indicating a crucial regulatory role for decorin and biglycan in the tooth mineralization.[2] Increased width of the enamel in the biglycan null teeth further indicated a repressor role in enamel mineralization (42).

The increased levels and distribution of biglycan and decorin in the predentin of *Dspp*−/− teeth indicate that the increased biglycan and decorin may play a crucial role in the formation of a defined mineralization front. The gap zones and their connected channels in the collagen fibrils are the predominant hydroxyapatite nucleation sites in the early mineralization stage (43, 44). Furthermore, it has been demonstrated that phosphophorin, a putative initiator of mineralization in dentin, is localized in the collagen fibril gap zones (45). Decorin binding to the gap zones of collagen fibril or near them may potentially block the mineralization sites and prevent interactions between collagen and the molecules that initiate mineralization (46).

It is also interesting to note that the *Dspp* products Dsp and Dpp, implicated in the tooth mineralization, could alter the levels of the proteoglycans. A number of factors have been known to regulate the expression of biglycan and decorin in a variety of tissues. TGF-$\beta$, a multi-functional cytokine, increases the levels of biglycan in MC3T3 cells (47). In an earlier study (22), we demonstrated down-regulation of Dspp expression in *Dspp*-TGF-$\beta$1 transgenic mice leading to dysplastic dentin. In these transgenic mice, we also observed elevated levels of biglycan and decorin by odontoblasts.[3] The elevated levels of proteoglycans in *Dspp*−/− mice and their distribution in the non-mineralized regions of teeth suggest that the *Dspp* gene products may control proteoglycans in the coronal regions of the dentin, where the mineralization process is complete. In addition, type I collagen levels in *Dspp*−/− teeth were unaffected. Therefore, we suggest that the increased levels of proteoglycans in the mutant mice interact with the collagen fibrils and promote the maturation process; however, they may fail to dissociate from the mature collagen required for subsequent dentin mineralization. This may be a result of either a reduced rate of their turnover, accelerated rate of synthesis (gene regulation), or a combination of both, contributing to the increased non-mineralized region. Therefore, we propose that *Dspp* gene products, in addition to their suggested role in the nucleation of mineralization, may play a pivotal role in regulation of proteoglycans during dentinogenesis. Overall, our results indicate that the absence of Dspp and the altered regulation of proteoglycans may be the causative factors that contribute to the mineralization defects in this disorder.

*Acknowledgments*—We thank Drs. Toshi Ohshima and Gulshan Sunawala for initial characterization of Dspp genomic clones and Drs. Henning Birkedal-Hansen, Mary Jo Danton, Larry Fisher, Yoshi Yamada, Marian Young, and Hynda Kleinman for helpful discussions and critical comments on the manuscript.

REFERENCES

1. Lumsden, A. G. (1988) *Development* **103,** (suppl.) 155–169
2. MacDougall, M., Zeichner-David, M., and Slavkin, H. C. (1985) *Biochem. J.* **232,** 493–500
3. MacDougall, M., Simmons, D., Luan, X., Nydegger, J., Feng, J., and Gu, T. T. (1997) *J. Biol. Chem.* **272,** 835–842
4. Feng, J. Q., Luan, X., Wallace, J., Jing, D., Ohshima, T., Kulkarni, A. B., D'Souza, R. N., Kozak, C. A., and MacDougall, M. (1998) *J. Biol. Chem.* **273,** 9457–9464
5. D'Souza, R. N., Bronckers, A. L., Happonen, R. P., Doga, D. A., Farach-Carson, M. C., and Butler, W. T. (1992) *J. Histochem. Cytochem.* **40,** 359–366
6. Begue-Kirn, C., Krebsbach, P. H., Bartlett, J. D., and Butler, W. T. (1998) *Eur. J. Oral Sci.* **106,** 963–970
7. D'Souza, R. N., Cavender, A., Sunavala, G., Alvarez, J., Ohshima, T., Kulkarni, A. B., and MacDougall, M. (1997) *J. Bone Miner. Res.* **12,** 2040–2049
8. Xiao, S., Yu, C., Chou, X., Yuan, W., Wang, Y., Bu, L., Fu, G., Qian, M., Yang, J., Shi, Y., Hu, L., Han, B., Wang, Z., Huang, W., Liu, J., Chen, Z., Zhao, G., and Kong, X. (2001) *Nat. Genet.* **27,** 201–204
9. Qin, C., Brunn, J. C., Cadena, E., Ridall, A., Tsujigiwa, H., Nagatsuka, H., Nagai, N., and Butler, W. T. (2002) *J. Dent. Res.* **81,** 392–394
10. Veis, A. (1993) *J. Bone Miner. Res.* **8,** Suppl. 2, S493–497
11. George, A., Bannon, L., Sabsay, B., Dillon, J. W., Malone, J., Veis, A., Jenkins, N. A., Gilbert, D. J., and Copeland, N. G. (1996) *J. Biol. Chem.* **271,** 32869–32873
12. Butler, W. T. (1998) *Eur. J. Oral Sci.* **106,** Suppl. 1, 204–210
13. Aplin, H. M., Hirst, K. L., Crosby, A. H., and Dixon, M. J. (1995) *Genomics* **30,** 347–349
14. MacDougall, M. (1998) *Eur. J. Oral Sci.* **106,** Suppl. 1, 227–233
15. Shields, E. D., Bixler, D., and el-Kafrawy, A. M. (1973) *Arch. Oral Biol.* **18,** 543–553
16. Rao, S., and Witkop, C. J., Jr. (1971) *Birth Defects Orig. Artic. Ser.* **7,** 153–184
17. Witkop, C. J., Jr., MacLean, C. J., Schmidt, P. J., and Henry, J. L. (1966) *Ala. J. Med. Sci.* **3,** 382–403
18. Levin, L. S., Leaf, S. H., Jelmini, R. J., Rose, J. J., and Rosenbaum, K. N. (1983) *Oral Surg. Oral Med. Oral Pathol.* **56,** 267–274
19. Zhang, X., Zhao, J., Li, C., Gao, S., Qiu, C., Liu, P., Wu, G., Qiang, B., Lo, W. H., and Shen, Y. (2001) *Nat. Genet.* **27,** 151–152
20. Rajpar, M. H., Koch, M. J., Davies, R. M., Mellody, K. T., Kielty, C. M., and Dixon, M. J. (2002) *Hum. Mol. Genet.* **11,** 2559–2565
21. Sreenath, T. L., Cho, A., MacDougall, M., and Kulkarni, A. B. (1999) *Int. J. Dev. Biol.* **43,** 509–516
22. Thyagarajan, T., Sreenath, T., Cho, A., Wright, J. T., and Kulkarni, A. B. (2001) *J. Biol. Chem.* **276,** 11016–11020
23. Smith, G., Smith, A. J., and Browne, R. M. (1988) *J. Oral Pathol.* **17,** 55–59
24. Fisher, L. W., Stubbs, J. T., 3rd, and Young, M. F. (1995) *Acta Orthop. Scand. Suppl.* **266,** 61–65
25. Balto, K., White, R., Mueller, R., and Stashenko, P. (2002) *Oral Surg. Oral Med. Oral Pathol. Oral Radiol. Endod.* **93,** 461–468
26. Bianco, P., Fisher, L. W., Young, M. F., Termine, J. D., and Robey, P. G. (1990) *J. Histochem. Cytochem.* **38,** 1549–1563
27. Takagi, M., Hishikawa, H., Hosokawa, Y., Kagami, A., and Rahemtulla, F. (1990) *J. Histochem. Cytochem.* **38,** 319–324
28. Yoshiba, N., Yoshiba, K., Iwaku, M., and Ozawa, H. (1996) *Arch. Oral Biol.* **41,** 351–357

[2] M. Young, unpublished data.

[3] T. Thyagarajan, unpublished data.

29. Embery, G., Hall, R., Waddington, R., Septier, D., and Goldberg, M. (2001) *Crit. Rev. Oral Biol. Med.* **12,** 331–349
30. Septier, D., Hall, R. C., Embery, G., and Goldberg, M. (2001) *Calcif. Tissue Int.* **69,** 38–45
31. Hocking, A. M., Shinomura, T., and McQuillan, D. J. (1998) *Matrix Biol.* **17,** 1–19
32. Hall, R., Septier, D., Embery, G., and Goldberg, M. (1999) *Histochem. J.* **31,** 761–770
33. Takagi, Y., Fujisawa, R., and Sasaki, S. (1986) *Connect. Tissue Res.* **14,** 279–292
34. Shokeir, M. H. (1972) *Clin. Genet.* **3,** 442–447
35. Kerebel, B., Daculsi, G., Menanteau, J., and Kerebel, L. M. (1981) *J. Dent. Res.* **60,** 1655–1660
36. Scott, J. E., and Dorling, J. (1965) *Histochemie* **5,** 221–233
37. Cam, Y., Lesot, H., Colosetti, P., and Ruch, J. V. (1997) *Arch. Oral Biol.* **42,** 385–391
38. Landis, W. J. (1999) *Gravit. Space Biol. Bull.* **12,** 15–26
39. Landis, W. J., Song, M. J., Leith, A., McEwen, L., and McEwen, B. F. (1993) *J. Struct. Biol.* **110,** 39–54
40. Hoshi, K., Kemmotsu, S., Takeuchi, Y., Amizuka, N., and Ozawa, H. (1999) *J. Bone Miner. Res.* **14,** 273–280
41. Boskey, A. L., Spevak, L., Doty, S. B., and Rosenberg, L. (1997) *Calcif. Tissue Int.* **61,** 298–305
42. Goldberg, M., Septier, D., Rapoport, O., Young, M., and Ameye, L. (2002) *J. Dent. Res.* **81,** 520–524
43. Weiner, S., and Traub, W. (1986) *FEBS Lett.* **206,** 262–266
44. Landis, W. J. (1986) *J. Ultrastruct. Mol. Struct. Res.* **94,** 217–238
45. Traub, W., Arad, T., and Weiner, S. (1992) *Matrix* **12,** 251–255
46. Raspanti, M., Alessandrini, A., Ottani, V., and Ruggeri, A. (1997) *J. Struct. Biol.* **119,** 118–122
47. Takeuchi, Y., Matsumoto, T., Ogata, E., and Shishiba, Y. (1993) *J. Bone Miner. Res.* **8,** 823–830